Protective effects of Bovine Serum Albumin on superparamagnetic iron oxide nanoparticles evaluated in the nematode *Caenorhabditis elegans*

Laura Gonzalez-Moragas, Si-Ming Yu, Elisa Carenza, Anna Laromaine, Anna Roig*

Institut de Ciència de Materials de Barcelona. Campus UAB. 08193 Bellaterra, Spain

KEYWORDS: *Caenorhabditis elegans*, Superparamagnetic Iron Oxide Nanoparticles, Bovine Serum Albumin, Nano-bio interfaces, Protein Corona, Surface Modification, Magnetometry.

ABSTRACT

Nanomaterials give rise to unique biological reactivity that need to be thoroughly investigated. The quest for enhanced magnetic nanomaterials of different shapes, magnetic properties or surface coatings continues for applications in drug delivery, targeting therapies, biosensing and magnetic separation. In this context, the use of simple *in vivo* models, such as *Caenorhabditis elegans,* to biologically evaluate nanoparticles is currently in increasing demand as it offers low-cost and information-rich experiments. In this work, we evaluated how surface modification (citrate and protein-coated) of superparamagnetic iron oxide nanoparticles (C-SPIONs and BSA-SPIONs respectively) induces changes in their toxicological profile and biodistribution using the animal model *Caenorhabditis elegans* and combining techniques from materials science and biochemistry. The acute toxicity and nanoparticle distribution were assessed in two populations of worms (adults and larvae) treated with both types of SPIONs. After 24 h treatment, nanoparticles were localized in the alimentary system of *C. elegans*; acute toxicity was stronger in adults and larvae exposed to citrate coated SPIONs (C-SPIONs) rather than Bovine Serum Albumin coated SPIONS (BSA-SPIONs). Adult uptake was similar for both SPION types whereas uptake in larvae was dependent on the surface coating, being higher for BSA-SPIONs. Nanoparticle size was evaluated upon excretion and a slight size decrease was found. Interestingly, all results indicate the protective effects of the BSA to prevent degradation of the nanoparticles and decrease acute toxicity to the worms, especially at high concentrations. We argue that this relevant information on the chemistry and toxicity of SPIONs *in vivo* could not be gathered using more classical *in vitro* approaches such as cell culture assays, thus endorsing the potential of *C. elegans* to assess nanomaterials at early stages of their synthetic formulations.

INTRODUCTION

The study of the interaction between nanoparticles (NPs) and biological environments has been the focus of recent investigations.[1-3] This evaluation is vital to improve the existing materials for biological applications, and to improve the design of biocompatible NPs that effectively carry out diagnostic, therapeutic or theranostic functions *in vivo*, and have a harmless toxicological profile.[4-5] In this line, detailed information about the effects of NP coating, their chemistry, the structure of the NPs, and their toxicity mechanisms are crucial to predict NPs behavior. [6-11] Surface modifications on NPs induce changes in their toxicological profile and behavior both *in vitro* and *in vivo*. For instance, magnetite (Fe_3O_4) cores (25 nm) functionalized with positive polyethyleneimine (PEI) and negative poly(acrylic acid) (PAA) did not show differences on the viability of human neuroblast SH-SY5Y cells, but the uptake of PEI NPs was 4.5-fold larger than PAA NPs after 2h incubation.[12] Polyvinylpirrolidone (PVP)-coated silver NPs (28 nm) reduced the reprotoxicity in *C. elegans*, and avoided NP transference to the growing embryo and in the subsequent generations compared to 1-nm citrate-coated silver NPs.[13] Sulfidation of PVP-coated silver NPs (37 nm) decreased the toxicity of silver NPs in zebrafish (*Danio rerio*).[14]

From the plethora of inorganic NPs available, superparamagnetic iron oxide NPs (SPIONs) show potential because of their biocompatibility and magnetic properties. SPIONs are approved by the US Food and Drug Administration as Magnetic Resonance Imaging (MRI) contrast agents and their application in magnetic hyperthermia is already at the clinical stage (phase II).[15-16] SPIONs are also investigated for drug delivery, targeting therapies, biosensing and magnetic separation to name only few applications.[17-18] Therefore the quest for enhanced magnetic nanomaterials of different shapes, magnetic properties or surface coatings continues.[19-20]

In order to facilitate the optimization of NPs and mitigate most of the difficulties associated with the use of complex animal models, we assessed the surface functionalization of superparamagnetic iron oxide nanoparticles (SPIONs) in *Caenorhabditis elegans (C. elegans*). The evaluation in simple animals at the early stages of the synthesis can reduce the number of candidate materials and facilitate the research before screening them in mammalian models minimizing ethical issues and avoiding high costs and delayed results.[21] *C. elegans* is a 1-mm-long soil nematode with a rapid-life cycle (3 days) and short lifespan (2-3 weeks) that is facile and inexpensive to grow.[22] Its small size and transparency permits the observation of NP uptake and distribution at the cellular, tissue and organism levels combining techniques and procedures from different fields such as materials science and biochemistry (Figure 1).[23-26] A detailed comparison of *C. elegans* and mammalian models can be found in the existing literature.[21, 27-28] Advantages and drawbacks of using *C. elegans* for the evaluation of nanomaterials are summarized in Figure 1D.

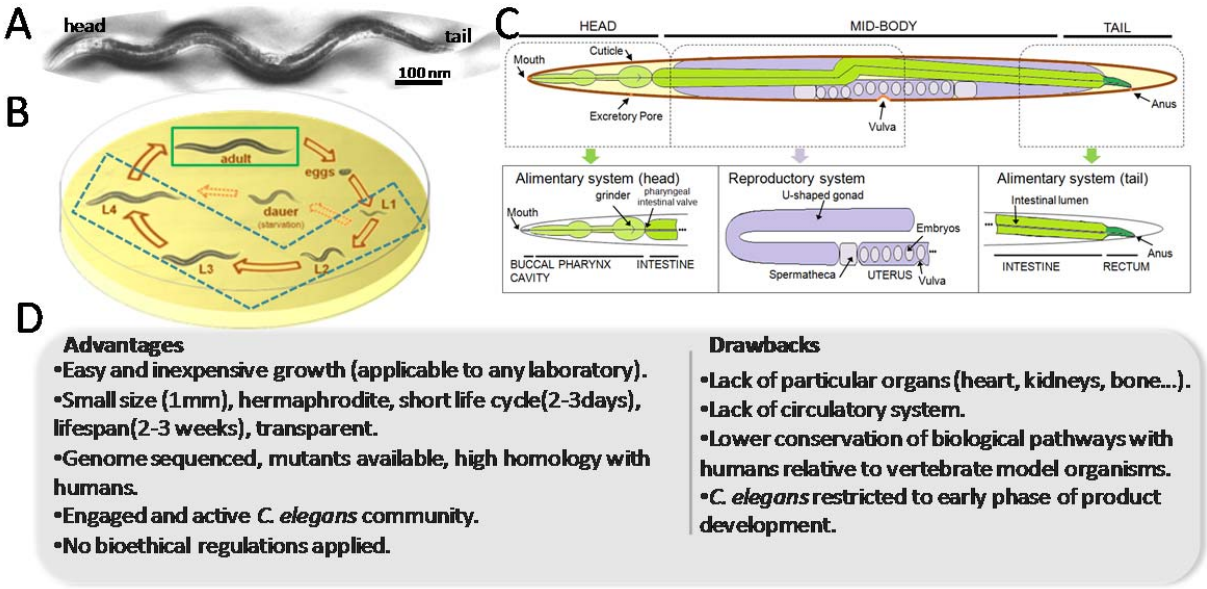

Figure 1. Main biological features of *C. elegans*. (A) Light microscopy image of *C. elegans*. (B) Life cycle progresses through four larval stages (L1–L4) before reaching adulthood. Larval stages are marked with a dotted blue box. Adults are marked with a green box. (C) General anatomy of *C. elegans*. (D) Table listing the advantages and drawbacks of working with *C. elegans*.

In this work, citrate coated SPIONs (C-SPIONs) and SPIONs coated with Bovine Serum Albumin (BSA-SPIONs) were chosen as a model system. The different surface functionalizations were investigated in order to determine whether they lead to different uptake, biodistribution or *in vivo* properties in adult and larvae populations of the model organism *C. elegans*.

MATERIALS AND METHODS

Materials

C. elegans Bristol strain N2 and *E. coli* OP50 were obtained from the *Caenorhabditis* Genetic Center (CGC) stock collection, University of Minnesota, St. Paul, MN, USA. Benzyl alcohol ≥99% was bought from Scharlau. Peptone, Yeast Extract, Bacteriological Agar and Tryptone were purchased from Conda Lab. All the other used reagents were bought from Sigma-Aldrich, if not stated otherwise.

Nanoparticle synthesis

Citrate-coated SPIONs (C-SPIONs) were synthesized by using microwave-assisted thermal decomposition, as described previously.[29] Iron (III) acetyl acetonate (0.35 mmol) was dissolved in anhydrous benzyl alcohol (4.5 ml) in a microwave tube and mixed with a vortex mixer for 30

s. The reaction tubes were transferred into a microwave CEM Discover reactor (Explorer 12-Hybrid; 2.45 GHz; 300 W). A heating ramp was used for 5 min at 60 ^{o}C and 10 min at 180 ^{o}C, before cooling to 50 ^{o}C in 3 min by using compressed nitrogen. Then, sodium citrate (150 µl; 10 wt.%) was added to each reaction tube and sonicated for 1 min. Acetone was added to precipitate the particles and centrifuged at 6000 rpm for 30 min. The supernatant was discarded and the washing step was repeated twice. The final black precipitate was dried overnight in an oven at 60 ^{o}C, and re-dispersed in MilliQ water (2 ml). The dispersion was adjusted to pH 7.4 by the addition of HNO_3 (0.1 M).

BSA-SPIONs were synthesized by using the BSA adsorption protocol described previously.[29] In brief, synthesized C-SPIONs were dispersed in MilliQ water (2 mg/ml). The dispersion was first adjusted to pH 11 by adding NaOH (0.01 M), and then equal volumes of the C-SPIONs dispersion (2 mg/ml) and BSA solution (5 mg/ml) were rapidly mixed and stirred with a vortex mixer for 10 min. Finally, the mixture was adjusted to pH 7.4 by adding HNO_3 solution (0.05 mM) and a BSA-SPIONs dispersion (1 mg/ml) was obtained.

To determine the iron concentration, C-SPIONs were sonicated for 10 min in an ultrasound bath. An aliquot of the sample was diluted with HCl (1%), and the iron content of the resulting solution was determined by flame absorption spectroscopy (air-acetylene) with a Perkin-Elmer 2100 spectrometer in triplicate. The concentration of SPIONs expressed throughout the text refers to the concentration of iron in the SPIONs.

Dynamic Light Scattering and Transmission Electron Microscopy analysis

Dynamic light scattering (DLS) and zeta potential measurements were performed with a Zetasizer Nano ZS (Malvern) with a He/Ne 633 nm laser at 25 ^{o}C. For each sample, three independent measurements were performed.

Transmission electron microscopy (TEM) samples were prepared by placing one drop of the corresponding SPION dispersion on the copper grid, blotting the copper grid with a filter paper and letting it evaporate completely at room temperature. C-SPIONs were imaged with a JEOL JEM-1210 electron microscope at an operating voltage of 120 KV. About 200 different particles were computed to depict the size distribution and the mean size of C-SPIONs.

Adsorption of BSA on C-SPIONs was visualized by performing negative staining TEM.[29] A drop of BSA-SPIONs was placed on a carbon-coated grid and then blotted with filter paper. Subsequently, uranyl acetate (5 μL; 2%) was placed on the grid for 1 min before being blotted. The grid was then placed in a 2011 JEOL electron microscope. About 200 different particles were counted to depict the size distribution and the mean size of the BSA-SPIONs.

Magnetometry

A magnetometer from Quantum Design MPMS5XL was used to perform magnetization measurements. Magnetization versus applied field was measured at 5 K after the material has been magnetically saturated up to 6 T. The zero field cooled-field cooled magnetization (ZFC-FC) was measured with a 50 Oe applied field in the range 4–300 K.

Worm growth and maintenance

Nematodes were grown on nematode growth medium (NGM) and fed *E. coli* OP50 according to the standard protocol at 20 ^{o}C.[38]

Preparation of the adult and larvae populations

Mix-staged well-fed worms with OP50 were rinsed with MilliQ water and transferred into a 15-ml centrifuge tube. Worms settle down in 10 min and then the supernatant was changed to clean MilliQ water. We washed the worms three times to remove any remaining bacteria. Adult worms were filtered by using a 40-µm pore-size nylon mesh (BD Falcon) and washed three times with MilliQ water to remove any remaining juvenile stages. The retentate worms were collected in MilliQ water and used as the adult population (less than 10% larvae). The filtrate was used as the larvae population.

Iron determination

Around 1 x 10^4 adults and 4 x 10^4 larvae in triplicate were treated with 500 µg SPIONs/ml for 24 h, transferred to a polycarbonate capsule, dried for 48 h at 60 ^{o}C, and used for magnetometry measurements. The quantity of SPIONs in the worms was evaluated by measuring the value of the remanence magnetization (M_R) at 5 K of the treated worms ($M_{R\ worms}$). The $M_{R\ worms}$ (emu) divided by the total number of worms gives the magnetization per worm (emu/worm). To know the amount of iron per worm, the magnetization per worm was divided by the value of the remanence magnetization of the SPIONs ($M_{R\ SPIONs}$) (emu/g Fe) also at 5 K. This value is not affected by any diamagnetic or paramagnetic components in the sample. Calculation was performed according to the following formula:

$$\text{NP uptake } \left(\frac{\text{pg Fe}}{\text{worm}}\right) = \frac{M_{R\ worms}\left(\frac{\text{emu}}{\text{worm}}\right)}{M_{R\ SPIONs}\left(\frac{\text{emu}}{\text{pg Fe}}\right)}$$

Nanoparticle uptake was normalized by worm body volume, dividing the NP uptake (pg Fe/worm) by the body volume of worms (either adults or larvae) expressed in nanoliters, as follows:

$$\text{NP uptake } \left(\frac{\text{pg Fe}}{\text{nl worm}}\right) = \frac{\text{NP uptake } \left(\frac{\text{pg Fe}}{\text{worm}}\right)}{\text{body volume (nl worm)}}$$

Scanning Electron Microscopy−Energy-dispersive X-ray spectroscopy analysis

A mix-staged worm population was treated with 500 µg SPIONs/ml for 24 h and fixed with 4% paraformaldehyde in MilliQ water for 2 h at room temperature. Fixed worms were washed three times with MilliQ water, and concentrated to 100 µl. A sample (20 µl) was transferred to a piece of carbon tape placed on a aluminum stub, and let it dry at room temperature. Scanning electron microscopy−energy-dispersive X-ray spectroscopy (SEM-EDX) analyses were carried out with a scanning electron microscope (QUANTA FEI 200 FEG-ESEM) equipped with an energy dispersive X-ray (EDX) system. SEM was used under low-vacuum conditions, an acceleration voltage of 10 kV, and an electron beam spot of 3.0.

Biodistribution assay

Two populations of worms (adults and larvae) were treated with 500 µg Fe/ml SPIONs for 24 h and fixed with 4% paraformaldehyde in MilliQ for 2 h at room temperature. Fixed worms were washed three times with MilliQ water, mounted on a glass slide and observed under the microscope. For Prussian blue staining, fixed worms were incubated with a mixture of Perl's solution (4% KFeCN : 4% HCl), incubated in the dark for 1 h and washed three times. The worms were then mounted on a glass slide and observed under the microscope. To study the

biodistribution of the SPIONs within the alimentary system of the treated worms, the alimentary system was divided into four segments —pharynx, anterior gut, central gut, and posterior gut— and the number of worms of the total 50 animals that presented SPIONs in the given segment was counted. Results were expressed as a percentage of worms with NPs in the pharynx, anterior gut, central-gut, and posterior-gut, respectively. Percentages of worms with NPs are represented as color map, establishing different intervals; 45-55%; pale orange, 55-65%light orange; 65-75%orange; 75-85%dark orange. Scale with colors and percentages are included in Figure 6.

Toxicological assays

We assessed two different parameters in order to evaluate the effects of SPIONs in *C. elegans:* survival and brood size. In the survival assay, the adult and larval populations were treated separately with C-SPIONs, BSA-SPIONs and $Fe(NO_3)_3$ in a final volume of 100 µl in 96-well plates for 24 h. The assay was performed in triplicate. The plates were tapped and the worms that moved were counted as alive. Each well contained between 9±3 adult worms and 25±8 larvae. The concentration range assayed was 0–500 µg/ml. To study the brood size, individual young adult worms non-treated and treated with C- and BSA-SPIONs (concentrations range: 100-500 µg/ml) were transferred to a NGM plate seeded with an OP50 lawn at 20 ^{o}C. The number of progeny was scored after 72 h of food resumption. Results are expressed as % of brood size in respect to the non-treated (control) worms. The reprotoxicity assay was performed per triplicate.

Release of the internalized SPIONs

After treatment with 500 µg Fe/ml SPIONs for 24 h, few adult worms were transferred to a NGM plate either with or without *E. coli* OP50. Plates were monitored for 12 h to check if food resumption or absence would induce excretion of the internalized SPIONs.

198 A mix-staged population consisting of 6 x 10^3 well-fed worms was treated with 500 µg Fe/ml
199 BSA-SPIONs and C-SPIONs in MilliQ water in a 24-well plate for 24 h. After treatment, worms
200 were collected in 1.5-ml eppendorfs, centrifuged at 1400 × g for 2 min, and the supernatant was
201 discarded. The worms were washed three times with MilliQ water to remove any remaining
202 SPIONs in the media. The worm pellet was diluted to 100 µl with MilliQ water, and incubated
203 with a freshly prepared mixture of household bleach (20 µl) and NaOH (5N; 1 : 1). After 20 min,
204 MilliQ water (1.5 ml) was added to stop the reaction, and the eppendorfs were centrifuged for 45
205 min at 14000 × g. After centrifugation, a brown pellet of NPs was visible at the bottom of the
206 eppendorf. The supernatant was removed, fresh MilliQ water was added up to a volume of 100
207 µl and the eppendorf was sonicated for 5 min. Finally, a drop was deposited onto a TEM grid
208 and observed with a JEOL JEM-1210 electron microscope at an operating voltage of 120 KV.
209 More than 100 different particles were measured to describe the size distribution and the mean
210 size of internalized C-SPIONs and BSA-SPIONs. Diluted C-SPIONs (100 µg/ml) were also
211 treated with bleach and used as control samples for the TEM observations.

212 To further characterize the effect of bleach treatment on the NPs, we monitored the changes in
213 the hydrodynamic mean diameter of diluted citrate SPIONs (100 µg/ml) by DLS before and after
214 the bleach treatment, and after NP re-dispersion.

215 **Magnetometry of the internalized SPIONs**

216 The dependence of the magnetic moment on the temperature (4–300 K) at an applied magnetic
217 field of 50 Oe was investigated for the superconducting quantum interference device samples
218 prepared as previously described. From the variation of the blocking temperature of the NPs

internalized inside the worms, their size decrease was calculated according to the Néel-Arrhenius equation:

$$\tau_N=\tau_0 \exp\left(\frac{KV}{k_B T}\right) \; ; \; V_2=\frac{V_1 T_{2B}}{T_{1B}} \; ; \%\text{decrease} = \frac{r_1 - r_2}{r_1} \cdot 100$$

in which τ_N is the Néel relaxation time; τ_0 is the attempt time; K is the magnetic anisotropy energy density; V is the NP volume; k_B is the Boltzmann constant; T is the temperature; T_B is the blocking temperature; r is the NP radius; 1 refers to as obtained NPs; 2 refers to the internalized NPs.

Statistical analysis

Past 3.03 was used for all statistical analyses. For the survival and brood size assays, statistical significance between groups was assessed using ANOVA followed by the Tukey's post hoc test. Survival and brood size data were fitted to four linear regression equations: adults/C-SPIONs, adults/BSA-SPIONs, larva/C-SPIONs, and larva/BSA-SPIONs. Differences between the behaviors of C- and BSA-SPIONs were studied using ANCOVA. For iron uptake, intergroup differences were assessed using Student's t-test, and the interaction between SPION type and *C. elegans* developmental stage was evaluated using a two-way ANOVA. Three levels of statistical significance were considered in all the cases: $p < 0.05$ (*), $p < 0.01$ (**) and $p < 0.001$ (***).

RESULTS AND DISCUSSION

Monodisperse C-SPIONs synthesized by using a microwave-assisted thermal decomposition method were characterized by TEM (Transmission Electron Microscopy), DLS (Dynamic Light Scattering), and zeta potential measurements. C-SPIONs had a diameter of 5.6 ± 0.8 nm, a hydrodynamic mean diameter of 17 nm, and a zeta potential of –41 mV. The same SPIONs when

protein coated (BSA-SPIONs) exhibited a hydrodynamic mean diameter of 25 nm and a zeta potential of –26 mV. TEM observations performed with negative staining and the increase in hydrodynamic diameter indicated that a single monolayer of BSA was coating the SPION surface (Figure 2).[29-30] We chose the BSA coating since it is well-known that the BSA can build a protein corona around NPs, stabilizing them, controlling their aggregation and improving their colloidal stability. Full characterization of the C-SPIONs and BSA-SPIONs are summarized in the Figure S1 and in the reference Yu et al.[29]

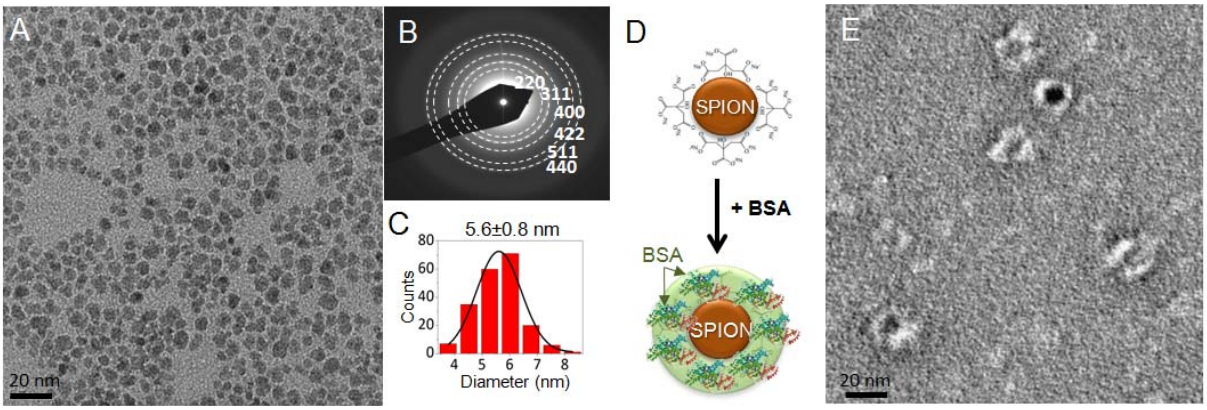

Figure 2. Characterization of SPIONs. (A) TEM image of C-SPIONs. (B) Diffraction pattern. (C) Histogram of TEM size distribution. (D) Scheme of BSA-SPION preparation. (E) Negative staining TEM image of BSA-SPIONs.

Previous studies of NPs in *C. elegans* have been mainly performed in solid media, mixing the NPs with the agar, but this exposure route bears high ionic strength and leads to NPs instability and precipitation, and uneven exposure of *C. elegans* to the NPs, increasing the variability and compromising the reproducibility of the results.[23, 31-35] Exposure of the worms to NPs in liquid media, as used in these experimental studies, can minimize the above-mentioned drawbacks.[23, 36]

In order to balance the stability of our NPs and the survival rate of *C. elegans,* we evaluated MilliQ water and M9 medium as *C. elegans* standard media. The high ionic strength of M9 medium promoted the aggregation of C-SPIONs, while in MilliQ water they remained stable, and the *C. elegans* survival was identical in both media after 24 h, therefore we selected MilliQ water as exposure media. The use of liquid media ensured the even distribution of NPs, a homogenous and free contact with the worms, and allowed us to monitor the physicochemical properties of the SPIONs during exposure, yielding reproducible results. *C. elegans* were exposed to SPIONs for 24 h without food, which allowed us to maintain the SPIONs inside the *C. elegans* intestine without being excreted.[32, 37] Prior to the incubation with NPs, *C. elegans* were fed on OP50 according to the standard practices.[38] The exclusion of bacteria during the incubation with NPs prevented that SPIONs were adsorbed on the bacteria, and avoided that the active metabolism of live bacteria could decrease the concentration of SPIONs and generate NP subproducts. Any potential starvation effects in the animals due to absence of food were taken into account with appropriate controls (Figure 3).

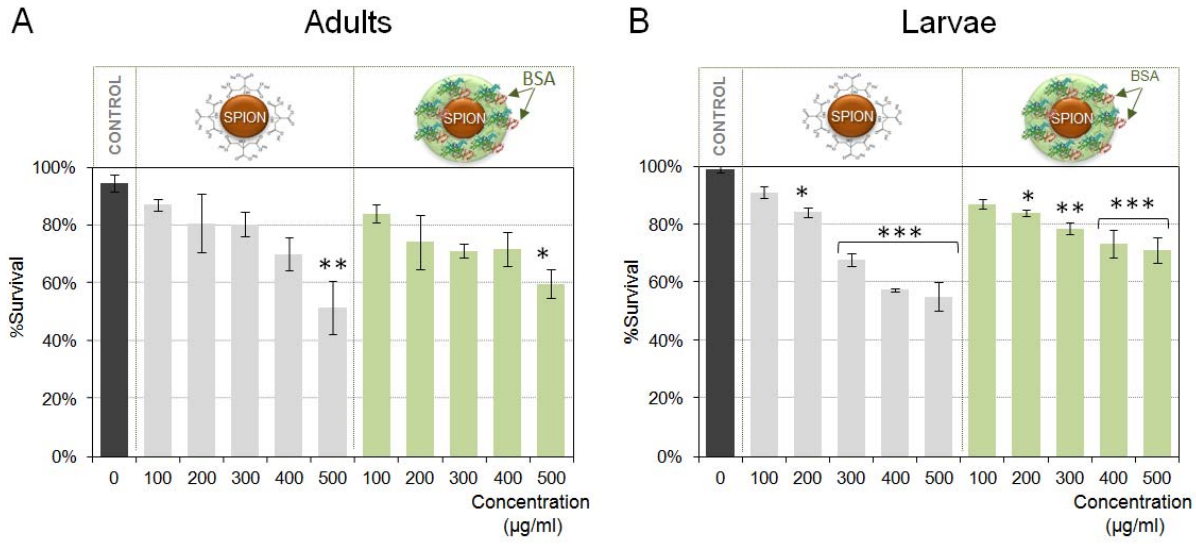

Figure 3. Effect of C-SPIONs and BSA-SPIONs on the acute toxicity of *C. elegans.* (A) Adult worms and (B) Larvae treated with 0–500 μg/ml C-SPIONs and BSA-SPIONs. Three replicates per concentration were performed. Error bars indicate standard error. $p < 0.05$ (*), $p < 0.01$ (**) and $p < 0.001$ (***).

We evaluated the survival rate in adult and larval populations of *C. elegans* treated with 0–500 μg/ml C-SPIONs and BSA-SPIONs after 24 h (Figure 3). The survival of adults at 24 h for both types of SPIONs was higher than 70% at doses below 400 μg/ml, and decreased significantly at 500 μg/ml to 60% ($p < 0.05$) and 51% ($p < 0.01$) in the case of BSA-SPIONs and C-SPIONs, respectively. In the case of larvae, survival was higher than 70% at all BSA-SPIONs concentrations, whereas the lethality of the C-SPIONs increased rapidly at concentrations > 200 μg/ml ($p < 0.05$). The higher sensitivity of larvae to SPION treatment could indicate that the toxic effects of SPIONs are stronger in the early stages of worms. Adult survival showed no differences in respect of the type of SPIONs, whereas statistical differences on larval survival were found at concentrations >400 μg/ml ($p<0.05$) depending on the treatment they received, either C-SPIONs or BSA-SPIONs. The survival of *C. elegans* after 24 h was fitted to linear regression, revealing a linear dose-response relationship of the short-term mortality over the range of concentrations studied (Table S1). The value of the slopes shows that the mortality increases quicker in the case of worms treated with C-SPIONs than in the case of treatment with BSA-SPIONs, although the differences are only statistically significant for larvae ($p<0.01$).

To investigate the influence of dissolved iron on the toxic effects of SPIONs, we studied the survival of *C. elegans* adult and larvae treated with Fe^{3+} at the same concentrations and time as for SPIONs exposure (Figure S2A). Under these conditions, neither dose-dependence between

294 the Fe^{3+} concentration and *C. elegans* mortality was observed, nor significant difference between
295 the survival of treated and control worms was noted. These results suggest that the toxicity
296 exerted by SPIONs cannot be explained solely by the release of metal ions, but SPIONs, at high
297 concentrations, must exert some toxicity through a nano-specific mechanism due to the small
298 size of the NPs, their high surface-area-to-volume ratio, or their high reactivity. The tolerance of
299 *C. elegans* to high concentrations of ferric ions may arise from the iron homeostasis of *the worm*,
300 which maintains cellular iron content within a narrow range to avoid the adverse consequences
301 of iron depletion or excess.[39]

302 Additionally, we evaluated the number of progeny in adults at the same concentrations that we
303 performed the survival assay as a sub-lethal endpoint. The brood size also indicated BSA-
304 SPIONs and C-SPIONs mildly affected *C. elegans* (Figure S3). Statistical differences between
305 treated and non-treated worms were found only at 500 μg/ml, which caused the higher decrease
306 on the number of progeny (brood size), 19% and 18% for the C-SPIONs and BSA-SPIONs
307 respectively. No statistical differences could be found between the effects of BSA-SPION and C-
308 SPION treatment on the brood size.

309 Hereinafter, we used 500 μg/ml as the exposure concentration for 24 h, since at this
310 concentration we found statistical differences between treated and control worms, and it allowed
311 us to visualize SPIONs inside the worms using an optical microscope. Exposure of worms for
312 shorter time (i.e. 6h) did not allow us to visualize the nanoparticles inside the *C. elegans.* As
313 mentioned, the use of MilliQ water as exposure media ensured that the colloidal stability of both
314 C-SPIONs and BSA-SPIONs was preserved upon incubation with *C. elegans* for 24 h (Figure
315 S4). Hence, our experimental design allowed us to perform controlled and well-characterized
316 exposures, which are parameters of vital importance to evaluate the interaction with NPs.[21]

317 In all cases, SPIONs were located in the alimentary tract, which indicates that SPIONs entered
318 the worms primarily through the intestinal tract by ingestion.[40] We studied SPION
319 biodistribution in treated worms by using Perl's Prussian blue to stain the iron present in
320 *C. elegans*, since it enhance its contrast and facilitate its visualization (Figure 4).[41] Interestingly,
321 the use of Prussian blue revealed the presence of SPIONs in areas in which they were not visible
322 by direct observation.

323

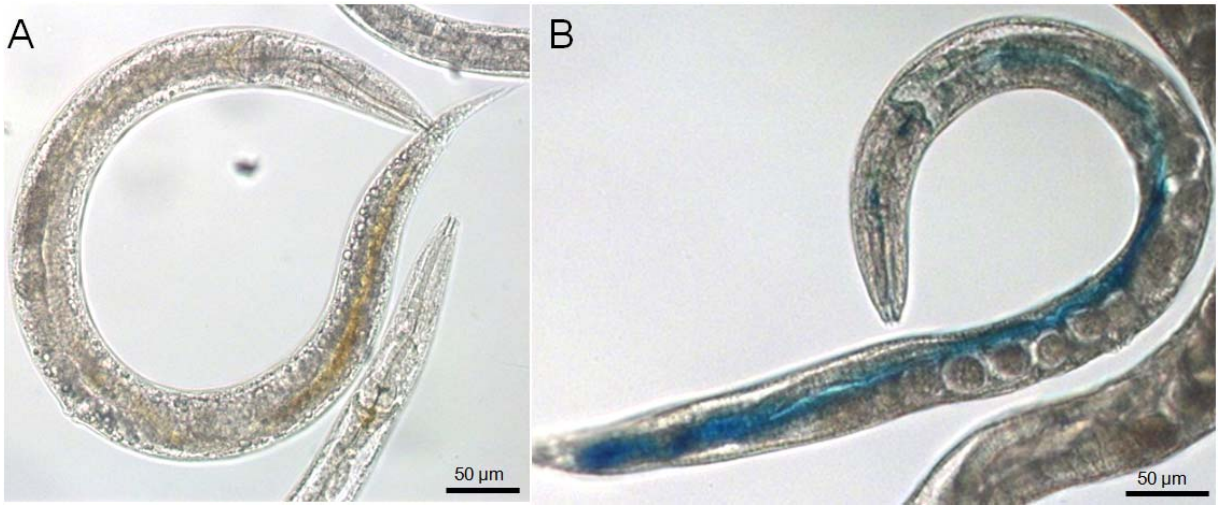

324

325 **Figure 4.** Light microscopy images of SPION-treated *C. elegans.* (A) Direct observation of C-
326 SPIONs inside fixed *C. elegans*. SPIONs appear brown. (B) Prussian blue stained worms where
327 BSA-SPIONs appear blue.

328

329 Translocation into the reproductory system was not observed within 24 h even though it has been
330 reported for several types of NPs, including gold, silica and silver NPs.[13, 35, 42] It is well-accepted
331 that enterocytes, the intestinal epithelial cells, have a limited endocytic capacity in both
332 *C. elegans* and mammals, therefore it supports the finding of absence of translocation through
333 this epithelial barrier.[43] The lack of translocation allows us to have a confined and astringent

environment in the *C. elegans* where we can evaluate the modification of our SPIONs for 24 h in such biological conditions.[32, 37] Entrance of SPIONs into the vulva by passive diffusion was observed in less than 5% of the worms (Figure S5), whereas for silica NPs it has been reported as a main entry pathway together with the pharynx.[34] Adsorption of SPIONs (either C- and BSA-SPIONS) in the cuticle of *C. elegans* [25] was discarded, since we did not detect iron in the *C. elegans* cuticle by EDX (Figure 5).

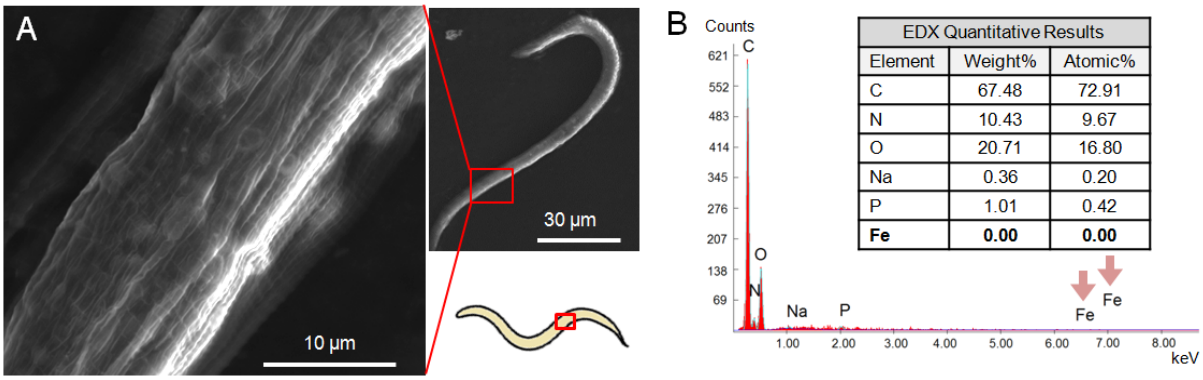

Figure 5. SEM-EDX analysis of treated *C. elegans*. (A) SEM image of treated *C. elegans* that does not show SPIONs adsorbed onto the cuticle. (B) A representative EDX measurement of the cuticle of treated *C. elegans.* The presence of iron is not detected in the cuticle of treated *C. elegans*.

More than 50 animals at both adult and larvae stages were stained with Prussian Blue and analyzed (Figure 6). We computed the predominance of SPIONs in the different regions (pharynx, anterior gut, central gut, posterior gut). Adults presented SPIONs in the pharynx region more frequently than larvae, independently of the SPION type. BSA-SPIONs were more homogenously distributed from the pharynx to the posterior gut in adults than C-SPIONs and

they were predominantly retained in the posterior gut relative to C-SPIONs in larvae, thus suggesting a more facile transit of BSA-SPIONs through the intestine

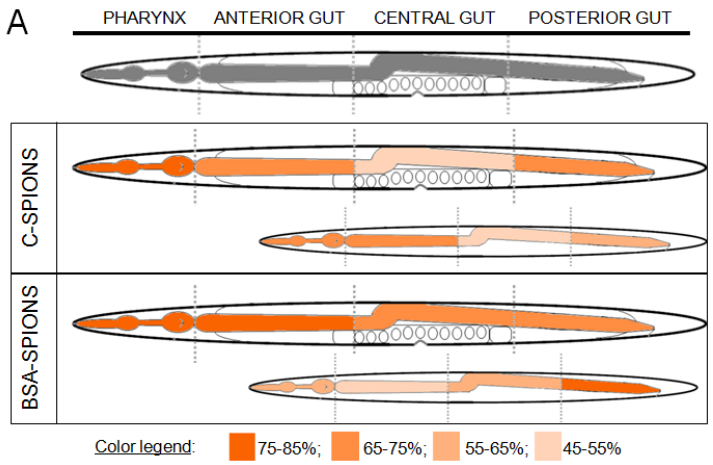

B

		Per worm (pg Fe/worm)	Per body volume (pg Fe/nl worm)
C-SPIONs	Adults	131±8	89±5
	Larvae	23±2	70±6
BSA-SPIONs	Adults	136±17	93±11
	Larvae	39±3	118±8

Figure 6. Biodistribution of C-SPIONs and BSA-SPIONs in adult and larval *C. elegans* after 24 h exposure to 500 µg/ml. (A) Scheme of the division of the alimentary system: pharynx, anterior gut, central gut, and posterior gut. Color map of the biodistribution of C-SPIONs and BSA-SPIONs in treated *C. elegans* adults and larvae. Color legend refers to the percentage of worms with NPs in the pharynx, anterior gut, central gut, and posterior-gut, respectively (of 50 animals per sample). Bright orange indicates a percentage of 75–85% of *C. elegans* with SPIONs present in that region, and light orange indicates a percentage of 45–55% of *C. elegans* with SPIONs present in that region of the all animals analyzed. (B) Iron content of *C. elegans* treated with 500 µg/ml during 24 h (n=3). The values are given with their standard deviation and relative errors.

We propose that, because BSA-SPIONs retain monodispersity for longer time, muscle contractions of *C. elegans* move BSA-SPIONs forward easily in the intestinal lumen relative to C-SPIONs (Figure 6A and Figure S6). Reported *in vitro* experiments using CaCO-2 cells,

intestinal epithelial cells, concluded that pretreatment of NPs with BSA reduced the adherence of the NPs to the cells by enhancing the NP colloidal stability and alleviating adherence.[44] In this line, cell studies of FDA-approved Abraxane®, an antitumoral active principle (paclitaxel) bound to human albumin, demonstrated that the presence of albumin facilitated the transport of paclitaxel through the endothelial cells, enhancing the accumulation of paclitaxel in the tumor.[45] Hence, BSA-coated NPs appear to interact less with biological environments than their non-coated counterparts, which could make BSA coating suitable for NPs as drug carriers because BSA-coated NPs could travel within an organism to reach specific tissues efficiently (quickly) and harmlessly (with low unspecific interactions).

The SPIONs uptake by *C. elegans* was quantified by using magnetometry. ZFC-FC plots showed that SPIONs kept their superparamagnetism after being internalized by the *C. elegans*. We measured the remanence magnetization of treated worms at 5 K (≈ 1 x 10^4 adults and ≈ 4 x 10^4 larvae per sample) after exposure to 500 μg/ml SPIONs for 24 h and compared these values to the remanence magnetization of SPIONs at the same temperature. The amount of iron uptake per worm showed dependence on the stage of the worms for both types of SPIONs ($p<0.001$) (Figure 6B) and was ≈ 4-6 times higher in adults than in larvae. Differences between the uptakes of the two types of SPIONs in adults were not significant (131 pg/worm for C-SPIONs and 136 pg/worm for BSA-SPIONs). However, larvae showed significant higher uptake of BSA-SPIONs (39 pg/worm) than C-SPIONs (23 pg/worm) ($p<0.01$).

Assuming that entrance of NPs into *C. elegans* occurs only through the alimentary system by ingestion, the lower NP uptake in larvae relative to adults may be attributed to differences in body and pharynx size. Larvae (L1-L4) are in average 2–3 times smaller than a newly molted adult with respect to both length and width, and 4.4 times smaller in volume.[46] Considering this,

we normalized NP uptake relative to body volume of adults and larvae, respectively. After normalization, BSA-SPIONs uptake remained slightly higher for adults than C-SPION uptake, and significantly higher for larvae ($p<0.01$) (Figures 6B and Table S2). The analysis of the two variables –developmental stage and SPION type– using a two-way ANOVA indicated that SPION type significantly influenced the NP uptake ($p<0.001$) whereas the development stage did not, thus reinforcing the influence of the BSA-coating on the NP uptake in *C. elegans*.

To investigate whether any modifications occurred to the NPs that had been internalized by *C. elegans* after 24 h, we analyzed the excreted NPs and the ZFC-FC plots in detail.

We transferred the magnetically treated worms onto Nematode Growth Medium plates with food, and within two minutes of food resumption, the worms began to excrete NPs through the anus in the form of micrometric agglomerates. SPIONs were excreted over a 2 h period (Figure 7A and Video S1).[32, 37, 47] In contrast, treated worms that were transferred to NGM plates without food still had SPIONs in their intestinal lumen after 12 h (Figure S7), which confirms that excretion is dependent upon food availability. In effect, we are able to modulate uptake and excretion of NPs in *C. elegans* based on the presence or absence of food source. Recovery of the internalized NPs in the treated worms was difficult because the excreted material was spread over the bacterial lawn and mixed with bacteria, which hindered their subsequent characterization. Therefore we adapted a standard bleaching procedure to dissolve the worm tissue and recover the internalized SPIONs (see Materials and Methods).[48] The procedure did not affect the initial size neither caused aggregation of SPIONs (Figure S8), thus any change in NP status could be attributed to interactions with *C. elegans*. We measured the diameter of internalized NPs by TEM (Figure 7B–7D) and analyzed over 100 particles. The diameter was

found to be smaller for C-SPIONs (10% reduction of the initial diameter; 0.6 nm), whereas for the BSA-SPIONs the diameter remained unchanged.

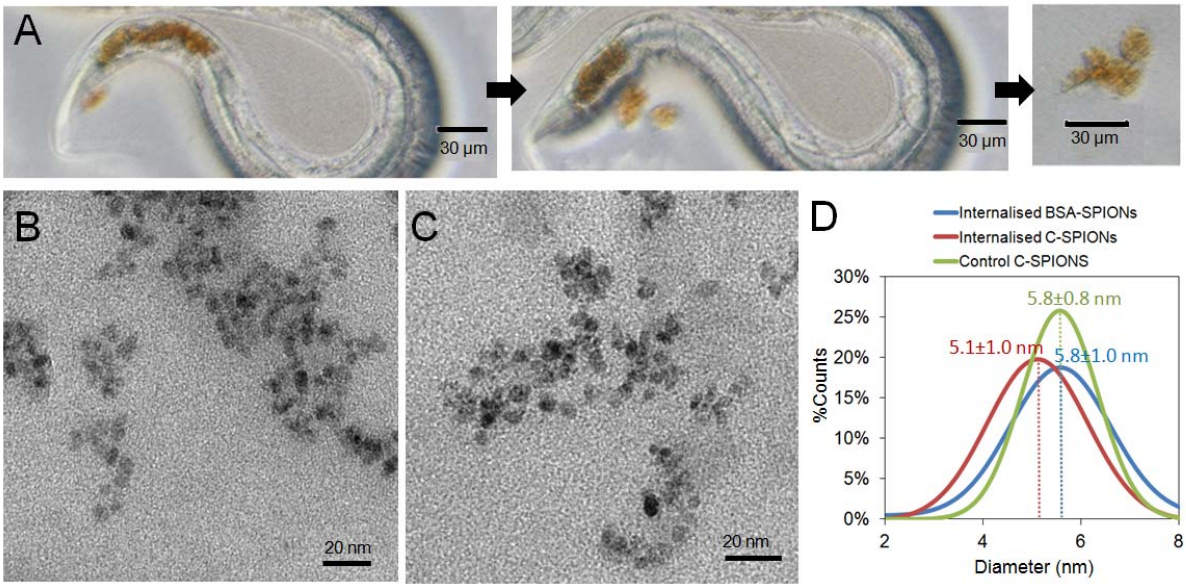

Figure 7. Characterization of internalized SPIONs. (A) Light microscopy images of excretion of SPIONs upon food resumption of treated *C. elegans*. (B) TEM image of internalized C-SPIONs. (C) TEM image of internalized BSA-SPIONs. (D) Gaussian distribution of TEM size for the internalized C-SPIONs, internalized BSA-SPIONs, and control C-SPIONs as-obtained.

ZFC-FC plots also showed that SPIONs decreased in diameter upon interaction with *C. elegans* of 14% and 6% for C-SPIONs and BSA-SPIONs respectively, calculated from the variation of the blocking temperatures, which correspond to the maximum value of the ZFC curve (Figure 8A). The size reduction was higher in adults than larvae for both types of SPIONs. The sharp increase of the FC curve at low temperatures indicated the presence of a paramagnetic component in the system, which could likely arise from the release of Fe^{3+} ions (Figure 8B). The

slight decrease in the size of the SPIONs and the subsequent release of Fe^{3+}could occur both during ingestion and intestinal residence time.

A

		$T_{B(worms)}$	$T_{B(SPIONs)}$	%decrease NP size
Adults	C-SPIONs	39 K	62 K	15%
	BSA-SPIONs	31 K	35 K	7%
Larvae	C-SPIONs	43 K	62 K	12%
	BSA-SPIONs	33 K	35 K	5%

B

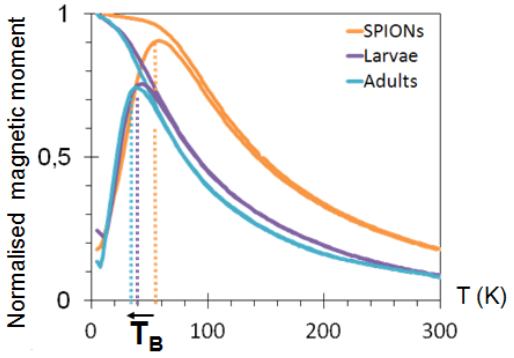

Figure 8. Characterization of internalized SPIONs from their blocking temperature. (A) The size decrease of internalized SPIONs can be calculated from the variation of the blocking temperatures of SPIONs upon interaction with *C. elegans.* (B) ZFC-FC graphs of control C-SPIONs and internalized C-SPIONs by adults and larvae.

In *C. elegans*, the buccal cavity and its associated structures act as a size selective filtering mechanism that efficiently trap bacteria (that is their food) into the pharynx. The particles trapped in the pharynx pass through the grinder.[49] Although the grinder impairs physical damage to bacterial cells (0.5–1 μm), polystyrene beads of up to 3 μm diameter appeared unaffected by their passage through the grinder.[40, 49] Hence, we hypothesize that size reduction of the SPIONs occurs during the residence time inside the gut because of the mild acidic conditions and the presence of digestive enzymes in the intestinal microenvironment, which results in their partial digestion. The acidity of the intestinal lumen of *C. elegans* ranges from pH 6, in the anterior pharynx, to pH 3.6 in the posterior intestine, and many digestive enzymes are secreted in the

443 anterior part of the gut including amylases, lipases, lysozymes, proteases, esterases and
444 nucleases.[28, 50] The acidic conditions in the posterior intestine could partially dissolve the C-
445 SPIONs and result in the release of Fe^{3+} ions.[51] Our results are consistent with those reported for
446 other metallic and metal oxide NPs in *C. elegans*.[52] Silver NPs of different sizes (3, 13, and 76
447 nm) and coatings (citrate and PVP) were toxic to *C. elegans* as a result of different mechanisms,
448 in which intraorganismal dissolved Ag was important.[13] Similar bioavailability of ZnO NPs and
449 $ZnCl_2$ also suggested that biotransformation (i.e. dissolution) occurred after ingestion of the NPs
450 by the worm.[36] After exposure to Cu NPs, an increase in the Cu^{+} concentration was also
451 detected, which suggests metabolism of the NPs.[31]

452 In the case of BSA-SPIONs, digestion of the protein layer is required before the iron oxide core
453 is accessible to the environmental conditions and contacts with the intestinal cells, which
454 suggests that BSA acts as a protective coating that prevents the direct interaction between
455 SPIONs and the biological environment, and thus decreases the potential toxicity of the
456 SPIONs.[53] *In vitro* experiments in simulated digestive fluid showed that although proteinases
457 could digest the BSA coating of nanoparticles, it still delayed the contact between the core of the
458 NP and the intestinal microenvironment, provided an additional barrier for diffusion and
459 decreased the accessibility or digestibility of NPs by digestive enzymes.[54] Similarly, our findings
460 indicate that the BSA coating improved the stability of SPIONs in the gastrointestinal tract of
461 *C. elegans* and protected BSA-SPIONs from digestion compared to C-SPIONs.

462 In conclusion, SPIONs exposure in liquid media allowed us to combine materials science,
463 chemistry and physical approaches to quantitatively assess the uptake and the modification of
464 SPIONs in *C. elegans* after 24 h. The different coatings of the SPIONs, citrate and BSA,
465 exhibited different short-term mortality and biodistribution in *C. elegans*. BSA-SPIONs were

466 associated with lower mortality than C-SPIONs in a broader range of concentrations, and more
467 remarkably at high concentrations, hence suggesting that the BSA coating layer has a protective
468 role not only for the material itself but also for the nematodes. The evaluation of the fate of
469 SPIONs within *C. elegans* was achieved due to the transparency of the worm and the staining
470 with Prussian Blue. SPIONs were localized only in the alimentary tract of the *C. elegans*
471 indicating ingestion as the main entry portal. BSA-SPIONs offered a more homogeneous
472 distribution within the alimentary tract of *C. elegans* compared to the C-SPIONs, which could be
473 attributed to their enhanced stability in biological environments and their reduced interaction
474 with the intestinal cells, as demonstrated in previous work.[29, 44] Therefore, if we aim to develop a
475 nanotherapeutic agent that should pass through the intestinal tract with minor biological
476 interactions, the BSA coating would rather facilitate this process.

477 Magnetometry allowed us to quantitatively compute the amount of SPIONs ingested by the
478 worms, which was higher for BSA-SPIONs in the two development stages under study. This
479 technique in combination with TEM let us evaluate the decrease in diameter for C-SPIONs
480 during digestion in the intestinal microenvironment of *C. elegans*. This size decrease was not
481 observed for the BSA-SPIONs, indicating the protective role of the BSA coating on the material
482 itself.

483 The results of this work open interesting avenues to evaluate different coatings of synthesized
484 NPs using *C. elegans* as an *in vivo* system in synthetic laboratories, by combining materials
485 science and chemistry. Future work will focus on the study of the molecular pathways triggered
486 by C-SPIONs and BSA-SPIONs to advance in the nanotoxicological mechanisms involved in
487 NPs with different coatings at different developmental stages of *C. elegans*.

ASSOCIATED CONTENT

Supporting Information. This material is available free of charge *via* the Internet at. It contains characterization of SPIONs before and after exposure to *C. elegans*, the instrumentation used for the characterization, additional images of the exposure of SPIONs with *C. elegans* and a video of the excretion of SPIONs by *C. elegans*.

AUTHOR INFORMATION

Corresponding Author

Anna Laromaine alaromaine@icmab.es

Author Contributions

Conceived and designed the experiments: AL, AR, LG. Performed the experiments: LG, SMY, EC. Analyzed the data: AL, AR, LG. Contributed reagents/materials/analysis tools: SMY, EC. Wrote the paper: AL, AR, LG.

Funding Sources

People Program (Marie Curie Actions) of the European Union's Seventh Framework Program (FP7/2007-2013) under REA grant agreement nº 303630. Spanish Ministry of Economy MAT 2012-35324. Generalitat de Catalunya 2014SGR213. COST Action MP1202. Ramon y Cajal grant RYC-2010-06082 (AL). China Scholarship Council fellowship (SMY, 201206150053). FPU fellowship (LGM, FPU12/05549) from the Spanish Ministry of Education.

ACKNOWLEDGMENT

C. elegans N2 and *E. coli* OP50 were provided by the CGC, which is funded by NIH Office of Research Infrastructure Programs (P40 OD010440). The research leading to these results has

509 received funding from the People Program (Marie Curie Actions) of the European Union's
510 Seventh Framework Program (FP7/2007-2013) under REA grant agreement nº 303630 and
511 cofounded by the European Social Fund. Authors acknowledge the funding from Spanish
512 Ministry of Economy MAT 2012-35324 and FEDER funds, the Generalitat de Catalunya
513 2014SGR213, the COST Action MP1202, Ramon y Cajal grant RYC-2010-06082 (AL), China
514 Scholarship Council fellowship (SMY, 201206150053), and FPU fellowship FPU12/05549
515 (LGM).

516
517 ABBREVIATIONS

518 BSA, Bovine Serum Albumin; BSA-SPIONs: BSA-coated SPIONs; CGC, Caenorhabditis
519 Genetic Center; C-SPIONs, citrate-coated SPIONs; DLS, Dynamic Light Scattering; EDX,
520 Energy-dispersive X-ray spectroscopy; M_R, Remanence Magnetization; NGM, Nematode growth
521 medium; MRI, Magnetic Resonance Imaging; NPs, Nanoparticles; NPs: Nanoparticles; PAA,
522 Poly(acrylic acid); PEI Polyethyleneimine; PVP, Polyvinylpirrolidone; SEM, Scanning electron
523 microscopy; SPIONs, Superparamagnetic iron oxide NPs; ZFC-FC, Zero field cooled-field
524 cooled magnetization.

525

526 REFERENCES

527 1. Monopoli, M. P.; Walczyk, D.; Campbell, A.; Elia, G.; Lynch, I.; Bombelli, F. B.;
528 Dawson, K. A., Physical-chemical aspects of protein corona: relevance to in vitro and in vivo
529 biological impacts of nanoparticles. *Journal of the American Chemical Society* **2011,** *133* (8),
530 2525-34. DOI: 10.1021/ja107583h.

2. Walczyk, D.; Bombelli, F. B.; Monopoli, M. P.; Lynch, I.; Dawson, K. A., What the Cell "Sees" in Bionanoscience. *Journal of the American Chemical Society* **2010,** *132* (16), 5761-5768. DOI: 10.1021/ja910675v.

3. Singh, R.; Nalwa, H. S., Medical Applications of Nanoparticles in Biological Imaging, Cell Labeling, Antimicrobial Agents, and Anticancer Nanodrugs. *Journal of Biomedical Nanotechnology* **2011,** *7* (4), 489-503. DOI: 10.1166/jbn.2011.1324.

4. Jain, T. K.; Reddy, M. K.; Morales, M. A.; Leslie-Pelecky, D. L.; Labhasetwar, V., Biodistribution, clearance, and biocompatibility of iron oxide magnetic nanoparticles in rats. *Molecular Pharmaceutics* **2008,** *5* (2), 316-327. DOI: 10.1021/mp7001285.

5. Reddy, L. H.; Arias, J. L.; Nicolas, J.; Couvreur, P., Magnetic Nanoparticles: Design and Characterization, Toxicity and Biocompatibility, Pharmaceutical and Biomedical Applications. *Chemical Reviews* **2012,** *112* (11), 5818-5878. DOI: 10.1021/cr300068p.

6. Krug, H. F.; Wick, P., Nanotoxicology: An Interdisciplinary Challenge. *ANGEWANDTE CHEMIE-INTERNATIONAL EDITION* **2011,** *50* (6), 1260-1278. DOI: 10.1002/anie.201001037.

7. Etheridge, M. L.; Campbell, S. A.; Erdman, A. G.; Haynes, C. L.; Wolf, S. M.; McCullough, J., The big picture on nanomedicine: the state of investigational and approved nanomedicine products. *Nanomedicine : nanotechnology, biology, and medicine* **2013,** *9* (1), 1-14. DOI: 10.1016/j.nano.2012.05.013.

8. Hassan, S.; Singh, A. V., Biophysicochemical perspective of nanoparticle compatibility: a critically ignored parameter in nanomedicine. *Journal of nanoscience and nanotechnology* **2014,** *14* (1), 402-14.

9. Saptarshi, S. R.; Duschl, A.; Lopata, A. L., Interaction of nanoparticles with proteins: relation to bio-reactivity of the nanoparticle. *Journal of nanobiotechnology* **2013,** *11*, 26. DOI: 10.1186/1477-3155-11-26.

10. Albanese, A.; Tang, P. S.; Chan, W. C., The effect of nanoparticle size, shape, and surface chemistry on biological systems. *Annual review of biomedical engineering* **2012,** *14*, 1-16. DOI: 10.1146/annurev-bioeng-071811-150124.

11. Wu, Q. L.; Li, Y. P.; Tang, M.; Wang, D. Y., Evaluation of Environmental Safety Concentrations of DMSA Coated Fe2O3-NPs Using Different Assay Systems in Nematode Caenorhabditis elegans. *PLoS One* **2012,** *7* (8). DOI: 10.1371/journal.pone.0043729.

12. Calatayud, M. P.; Sanz, B.; Raffa, V.; Riggio, C.; Ibarra, M. R.; Goya, G. F., The effect of surface charge of functionalized Fe3O4 nanoparticles on protein adsorption and cell uptake. *Biomaterials* **2014,** *35* (24), 6389-99. DOI: 10.1016/j.biomaterials.2014.04.009.

13. Meyer, J. N.; Lord, C. A.; Yang, X. Y.; Turner, E. A.; Badireddy, A. R.; Marinakos, S. M.; Chilkoti, A.; Wiesner, M. R.; Auffan, M., Intracellular uptake and associated toxicity of silver nanoparticles in Caenorhabditis elegans. *Aquatic Toxicology* **2010,** *100* (2), 140-50. DOI: 10.1016/j.aquatox.2010.07.016.

14. Levard, C.; Hotze, E. M.; Colman, B. P.; Dale, A. L.; Truong, L.; Yang, X. Y.; Bone, A. J.; Brown, G. E., Jr.; Tanguay, R. L.; Di Giulio, R. T.; Bernhardt, E. S.; Meyer, J. N.; Wiesner, M. R.; Lowry, G. V., Sulfidation of silver nanoparticles: natural antidote to their toxicity. *Environmental science & technology* **2013,** *47* (23), 13440-8. DOI: 10.1021/es403527n.

15. Christen, T.; Ni, W.; Qiu, D.; Schmiedeskamp, H.; Bammer, R.; Moseley, M.; Zaharchuk, G., High-resolution cerebral blood volume imaging in humans using the blood pool contrast agent ferumoxytol. *Magnetic resonance in medicine : official journal of the Society of*

575 *Magnetic Resonance in Medicine / Society of Magnetic Resonance in Medicine* **2012**. DOI:
576 10.1002/mrm.24500.
577 16. Laurent, S.; Dutz, S.; Haefeli, U. O.; Mahmoudi, M., Magnetic fluid hyperthermia: Focus
578 on superparamagnetic iron oxide nanoparticles. *Advances in Colloid and Interface Science* **2011,**
579 *166* (1-2), 8-23. DOI: 10.1016/j.cis.2011.04.003.
580 17. Shubayev, V. I.; Pisanic, T. R., II; Jin, S., Magnetic nanoparticles for theragnostics.
581 *Advanced Drug Delivery Reviews* **2009,** *61* (6), 467-477. DOI: 10.1016/j.addr.2009.03.007.
582 18. Veiseh, O.; Gunn, J. W.; Zhang, M., Design and fabrication of magnetic nanoparticles for
583 targeted drug delivery and imaging. *Advanced Drug Delivery Reviews* **2010,** *62* (3), 284-304.
584 DOI: 10.1016/j.addr.2009.11.002.
585 19. Hao, R.; Xing, R.; Xu, Z.; Hou, Y.; Gao, S.; Sun, S., Synthesis, Functionalization, and
586 Biomedical Applications of Multifunctional Magnetic Nanoparticles. *Advanced Materials* **2010,**
587 *22* (25), 2729-2742. DOI: 10.1002/adma.201000260.
588 20. Mahmoudi, M.; Sant, S.; Wang, B.; Laurent, S.; Sen, T., Superparamagnetic iron oxide
589 nanoparticles (SPIONs): Development, surface modification and applications in chemotherapy.
590 *Advanced Drug Delivery Reviews* **2011,** *63* (1-2), 24-46. DOI: 10.1016/j.addr.2010.05.006.
591 21. Gonzalez-Moragas, L.; Roig, A.; Laromaine, A., C. elegans as a tool for in vivo
592 nanoparticle assessment. *Advances in Colloid and Interface Science* (0). DOI:
593 http://dx.doi.org/10.1016/j.cis.2015.02.001.
594 22. Wood, W. B., *The Nematode Caenorhabditis Elegans*. Cold Spring Harbor Laboratory:
595 1988.

596 23. Kim, S. W.; Nam, S.-H.; An, Y.-J., Interaction of Silver Nanoparticles with Biological
597 Surfaces of Caenorhabditis elegans. *Ecotoxicology and Environmental Safety* **2012,** *77*, 64-70.
598 DOI: 10.1016/j.ecoenv.2011.10.023.
599 24. Wu, Q.; Li, Y.; Li, Y.; Zhao, Y.; Ge, L.; Wang, H.; Wang, D., Crucial role of the
600 biological barrier at the primary targeted organs in controlling the translocation and toxicity of
601 multi-walled carbon nanotubes in the nematode Caenorhabditis elegans. *Nanoscale* **2013,** *5* (22),
602 11166-78. DOI: 10.1039/c3nr03917j.
603 25. Kaletta, T.; Hengartner, M. O., Finding function in novel targets: C. elegans as a model
604 organism. *Nature reviews. Drug discovery* **2006,** *5* (5), 387-98. DOI: 10.1038/nrd2031.
605 26. Wu, Q.; Yin, L.; Li, X.; Tang, M.; Zhang, T.; Wang, D., Contributions of altered
606 permeability of intestinal barrier and defecation behavior to toxicity formation from graphene
607 oxide in nematode Caenorhabditis elegans. *Nanoscale* **2013,** *5* (20), 9934-43. DOI:
608 10.1039/c3nr02084c.
609 27. Corsi, A. K., A Biochemist's Guide to C. elegans. *Analytical biochemistry* **2006,** *359* (1),
610 1-17. DOI: 10.1016/j.ab.2006.07.033.
611 28. Hall, D. H.; Altun, Z. F., *C. Elegans Atlas*. Cold Spring Harbor Laboratory Press: 2008.
612 29. Yu, S. M.; Laromaine, A.; Roig, A., Enhanced stability of superparamagnetic iron oxide
613 nanoparticles in biological media using a pH adjusted-BSA adsorption protocol. *J. Nanopart.*
614 *Res.* **2014,** *16* (7). DOI: 10.1007/s11051-014-2484-1.
615 30. Rocker, C.; Potzl, M.; Zhang, F.; Parak, W. J.; Nienhaus, G. U., A quantitative
616 fluorescence study of protein monolayer formation on colloidal nanoparticles. *Nature*
617 *Nanotechnology* **2009,** *4* (9), 577-580. DOI: 10.1038/nnano.2009.195.

618 31. Gao, Y.; Liu, N.; Chen, C.; Luo, Y.; Li, Y.; Zhang, Z.; Zhao, Y.; Zhao, B.; Iida, A.; Chai,
619 Z., Mapping technique for biodistribution of elements in a model organism, Caenorhabditis
620 elegans, after exposure to copper nanoparticles with microbeam synchrotron radiation X-ray
621 fluorescence. *Journal of Analytical Atomic Spectrometry* **2008,** *23* (8), 1121-1124. DOI:
622 10.1039/b802338g.
623 32. Mohan, N.; Chen, C. S.; Hsieh, H. H.; Wu, Y. C.; Chang, H. C., In vivo imaging and
624 toxicity assessments of fluorescent nanodiamonds in Caenorhabditis elegans. *Nano letters* **2010,**
625 *10* (9), 3692-9. DOI: 10.1021/nl1021909.
626 33. Qu, Y.; Li, W.; Zhou, Y.; Liu, X.; Zhang, L.; Wang, L.; Li, Y. F.; Iida, A.; Tang, Z.;
627 Zhao, Y.; Chai, Z.; Chen, C., Full assessment of fate and physiological behavior of quantum dots
628 utilizing Caenorhabditis elegans as a model organism. *Nano letters* **2011,** *11* (8), 3174-83. DOI:
629 10.1021/nl201391e.
630 34. Scharf, A.; Piechulek, A.; von Mikecz, A., Effect of Nanoparticles on the Biochemical
631 and Behavioral Aging Phenotype of the Nematode Caenorhabditis elegans. *Acs Nano* **2013,** *7*
632 (12), 10695-10703. DOI: 10.1021/nn403443r.
633 35. Pluskota, A.; Horzowski, E.; Bossinger, O.; von Mikecz, A., In Caenorhabditis elegans
634 Nanoparticle-Bio-Interactions Become Transparent: Silica-Nanoparticles Induce Reproductive
635 Senescence. *PLoS One* **2009,** *4* (8), e6622. DOI: 10.1371/journal.pone.0006622.
636 36. Ma, H.; Bertsch, P. M.; Glenn, T. C.; Kabengi, N. J.; Williams, P. L., Toxicity of
637 manufactured zinc oxide nanoparticles in the nematode *Caenorhabditis elegans*. *Environmental*
638 *Toxicology and Chemistry* **2009,** *28* (6), 1324-1330.

37. Lim, S. F.; Riehn, R.; Ryu, W. S.; Khanarian, N.; Tung, C. K.; Tank, D.; Austin, R. H., In vivo and scanning electron microscopy imaging of upconverting nanophosphors in Caenorhabditis elegans. *Nano letters* **2006,** *6* (2), 169-174. DOI: 10.1021/nl0519175.

38. Brenner, S., The genetics of Caenorhabditis elegans. *Genetics* **1974,** *77* (1), 71-94.

39. Anderson, C. P.; Leibold, E. A., Mechanisms of iron metabolism in Caenorhabditis elegans. *Frontiers in pharmacology* **2014,** *5*, 113. DOI: 10.3389/fphar.2014.00113.

40. Fang-Yen, C.; Avery, L.; Samuel, A. D., Two size-selective mechanisms specifically trap bacteria-sized food particles in Caenorhabditis elegans. *Proceedings of the National Academy of Sciences of the United States of America* **2009,** *106* (47), 20093-6. DOI: 10.1073/pnas.0904036106.

41. Carenza, E.; Barcelo, V.; Morancho, A.; Levander, L.; Boada, C.; Laromaine, A.; Roig, A.; Montaner, J.; Rosell, A., In vitro angiogenic performance and in vivo brain targeting of magnetized endothelial progenitor cells for neurorepair therapies. *Nanomedicine : nanotechnology, biology, and medicine* **2014,** *10* (1), 225-34. DOI: 10.1016/j.nano.2013.06.005.

42. Kim, S. W.; Kwak, J. I.; An, Y.-J., Multigenerational Study of Gold Nanoparticles inCaenorhabditis elegans: Transgenerational Effect of Maternal Exposure. *Environmental science & technology* **2013,** *47* (10), 5393-5399. DOI: 10.1021/es304511z.

43. Audus, K. L.; Raub, T. J., *Biological Barriers to Protein Delivery*. Springer US: 1993. DOI: 10.1007/978-1-4615-2898-2.

44. Sinnecker, H.; Ramaker, K.; Frey, A., Coating with luminal gut-constituents alters adherence of nanoparticles to intestinal epithelial cells. *Beilstein Journal of Nanotechnology* **2014,** *5*, 2308-2315. DOI: 10.3762/bjnano.5.239.

661 45. Dosio, F.; Brusa, P.; Crosasso, P.; Arpicco, S.; Cattel, L., Preparation, characterization
662 and properties in vitro and in vivo of a paclitaxel-albumin conjugate. *Journal of Controlled*
663 *Release* **1997,** *47* (3), 293-304. DOI: 10.1016/s0168-3659(97)01656-8.
664 46. Knight, C. G.; Patel, M. N.; Azevedo, R. B.; Leroi, A. M., A novel mode of ecdysozoan
665 growth in Caenorhabditis elegans. *Evolution & development* **2002,** *4* (1), 16-27.
666 47. Laaberki, M. H.; Dworkin, J., Role of spore coat proteins in the resistance of Bacillus
667 subtilis spores to Caenorhabditis elegans predation. *Journal of bacteriology* **2008,** *190* (18),
668 6197-203. DOI: 10.1128/JB.00623-08.
669 48. Stiernagle, T., Maintenance of C. elegans. In *WormBook*, Community, T. C. e. R., Ed.
670 WormBook. DOI: 10.1895/wormbook.1.101.1.
671 49. Avery, L.; You, Y.-J., C. elegans feeding. In *WormBook*, Community, T. C. e. R., Ed.
672 WormBook. DOI: 10.1895/wormbook.1.150.1.
673 50. Chauhan, V. M.; Orsi, G.; Brown, A.; Pritchard, D. I.; Aylott, J. W., Mapping the
674 Pharyngeal and Intestinal pH of Caenorhabditis elegans and Real-Time Luminal pH Oscillations
675 Using Extended Dynamic Range pH-Sensitive Nanosensors. *Acs Nano* **2013,** *7* (6), 5577-5587.
676 DOI: 10.1021/nn401856u.
677 51. Huang, G.; Chen, H.; Dong, Y.; Luo, X.; Yu, H.; Moore, Z.; Bey, E. A.; Boothman, D.
678 A.; Gao, J., Superparamagnetic iron oxide nanoparticles: amplifying ROS stress to improve
679 anticancer drug efficacy. *Theranostics* **2013,** *3* (2), 116-26. DOI: 10.7150/thno.5411.
680 52. Zhao, Y.; Wu, Q.; Li, Y.; Wang, D., Translocation, transfer, and in vivo safety evaluation
681 of engineered nanomaterials in the non-mammalian alternative toxicity assay model of nematode
682 Caenorhabditis elegans. *Rsc Advances* **2013,** *3* (17), 5741-5757. DOI: 10.1039/c2ra22798c.

683 53. Malvindi, M. A.; De Matteis, V.; Galeone, A.; Brunetti, V.; Anyfantis, G. C.;
684 Athanassiou, A.; Cingolani, R.; Pompa, P. P., Toxicity assessment of silica coated iron oxide
685 nanoparticles and biocompatibility improvement by surface engineering. *PLoS One* **2014,** *9* (1),
686 e85835. DOI: 10.1371/journal.pone.0085835.
687 54. Li, Z.; Ha, J.; Zou, T.; Gu, L., Fabrication of coated bovine serum albumin (BSA)-
688 epigallocatechin gallate (EGCG) nanoparticles and their transport across monolayers of human
689 intestinal epithelial Caco-2 cells. *Food & Function* **2014,** *5* (6), 1278-1285. DOI:
690 10.1039/c3fo60500k.

691

692 Table of Contents Graphic

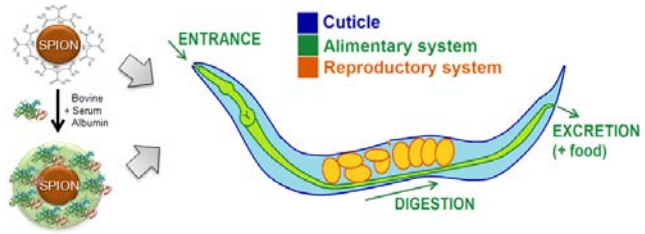

693